

Cu₂ZnSn(S_xSe_{1-x})₄ Thin-Film Solar Cells Utilizing Simultaneous Reaction of a Metallic Precursor with Elemental Sulfur and Selenium Vapor Sources

Noritaka Momose*, Myo Than Htay¹, Kazuki Sakurai¹, Shota Iwano¹, Yoshio Hashimoto¹, and Kentaro Ito¹

Department of Electrical and Electronic Engineering, Nagano National College of Technology, Nagano 381-8550, Japan

¹*Department of Electrical and Electronic Engineering, Faculty of Engineering, Shinshu University, Nagano 380-8553, Japan*

A Cu₂ZnSn(S_xSe_{1-x})₄ (CZTSSe) solid alloy was prepared by reacting a metallic precursor with sulfur and selenium in a closed tube simultaneously. It was confirmed that the CZTSSe alloy could be synthesized over the whole compositional range and its lattice transformation was in good agreement with Vegard's law. The crystal grain size and electrical conductivity were enhanced when the selenium content was increased. In a CdS/CZTSSe heterojunction solar cell, the photovoltaic efficiency was improved due to the enhancement of the short-circuit current in accordance with the narrowing of the optical bandgap of the CZTSSe absorber.

Environment-friendly Cu₂ZnSnS₄ (CZTS), which has a direct bandgap of about 1.5 eV and a high absorption coefficient above 10⁴ cm⁻¹, has been considered as a candidate material for future photovoltaic applications since one of the present authors and Nakazawa reported experimental results that verified its potential as a thin-film solar absorber in 1988.^{1,2)} Since then, Katagiri *et al.* reported a CdS/CZTS junction solar cell with a photovoltaic conversion efficiency of 6.7%,³⁾ which was followed by Shin *et al.* with a higher efficiency of 8.4% proving that the CZTS is a promising photovoltaic material.⁴⁾ In addition to these, Barkhouse *et al.* reported a breaking record of efficiency of over 10% based on a Cu₂ZnSn(S_xSe_{1-x})₄ (CZTSSe) alloy that assured its potential for practical applications.⁵⁾ Up to now, the thin films of CZTS and its related alloy of CZTSSe were prepared by various techniques such as vacuum deposition method,^{6,7)} solution-based method,^{8,9)} etc.^{10,11)} We previously prepared the CZTS thin films by sulfurization of metallic precursors under elemental sulfur ambient in a sealed tube.^{12,13)} The merits of this technique are as follows: (1) only inexpensive metallic sources are required, (2) rapid fabrication is realized, and (3) it can be integrated into a conventional in-line production system for large-scale photovoltaic applications.^{14,15)} In this paper, we proposed a simultaneous reaction method for fabricating the thin films of CZTSSe alloy with controlled composition. The material properties of the CZTSSe thin films and photovoltaic characteristics of the CdS/CZTSSe junction solar cell were also discussed.

*E-mail address: momose@nagano-nct.ac.jp

To prepare a CZTSSe thin film, a metallic precursor of Cu-Zn-Sn, which was simultaneously sputtered on a soda-lime glass substrate, was used. The precursors were set to 0.65 μm in thickness and the compositional ratios were adjusted to $\text{Cu}/(2\text{Zn}) = 0.75$, $\text{Cu}/(2\text{Sn}) = 0.90$, and $\text{Zn}/\text{Sn} = 1.2$. The resultant metallic compositions of the CZTSSe films were within 5% to those of the precursors. The precursors were sealed in a glass tube (base pressure was about 5 mPa) together with the powders of elemental sulfur and/or selenium, and then annealed at 520 $^{\circ}\text{C}$ for 15 min. During the annealing, rapid thermal elevation (310 $^{\circ}\text{C}$ per min) was applied, followed by natural cooling after the reaction period of 15 min. The details of the sputtering and annealing apparatuses are described in our previous report.¹²⁾ The compositional ratio of sulfur and selenium in the CZTSSe alloy was controlled by means of the ratio of sulfur and selenium partial vapor pressures at a desired annealing temperature in the closed tube. The ratio of partial vapor pressures was adjusted using the ratio of enclosed sulfur and selenium powders. In this technique, the final resultant of $\text{Se}/(\text{S}+\text{Se})$ ratio in the CZTSSe alloy was close to that of the preset partial vapor pressure ratio during the annealing process.

The surface morphology of the absorber films and the cross-sectional image of the cells were observed by field emission scanning electron microscopy. The composition of the films was determined by energy-dispersive X-ray spectroscopy (EDX). X-ray diffractometry (XRD) was used for material identification and evaluation of the crystalline properties. A four-probe method was employed for measuring the resistivity. To evaluate the photovoltaic properties, solar cells with $\text{In}_2\text{O}_3/\text{CdS}/\text{CZTSSe}/\text{Mo}/\text{SLG}$ structure were fabricated by the same processes as in our previous report.¹²⁾ The In_2O_3 film with a resistivity of $3 \times 10^{-4} \Omega \cdot \text{cm}$ was deposited by RF magnetron sputtering of a non-doped In_2O_3 target under pure Ar ambient without heating the substrate. The solar cell characteristics (J - V curve) were measured under an AM 1.5 radiation with 100 mW/cm^2 . The active area of each cell was 2.25 mm^2 . A spectrophotometer was used for measuring the quantum efficiency (QE) of the cell.

The XRD patterns of CZTSSe thin films with various $\text{Se}/(\text{S}+\text{Se})$ ratios are shown in Fig. 1. The patterns of the samples that have the $\text{Se}/(\text{S}+\text{Se})$ ratio of 0 [CZTS only] and 1 [$\text{Cu}_2\text{ZnSnSe}_4$ (CZTSe) only] are in good agreement with that of the JCPDS patterns for CZTS (26-0575) and CZTSe (70-8930), respectively. From these results, it can be considered that both CZTS and CZTSe have similar crystal structures, which might be ascribed to at least either one of the following: kesterite, stannite or partially disordered kesterite.¹⁶⁾ In the cases of samples that contained both sulfur and selenium, all the diffraction peaks were located between the patterns of CZTS and CZTSe. The peak shifting of these patterns due to the transformation of the lattice spacing by different compositional ratios of sulfur and selenium was also confirmed. The XRD peaks that can be assigned as the diffraction patterns of SnS_2 and SnSe_2 phases were also detected in the CZTS and CZTSe, respectively. By X-ray photoelectron spectroscopy analysis, a distinct gradient of $\text{Se}/(\text{Se}+\text{S})$ ratio along the film's depth was not confirmed. However, a gradient of Sn with higher concentration at the surface was observed. The excess of Sn composition at the surface could be explained if SnS_2 and SnSe_2 phases, which were

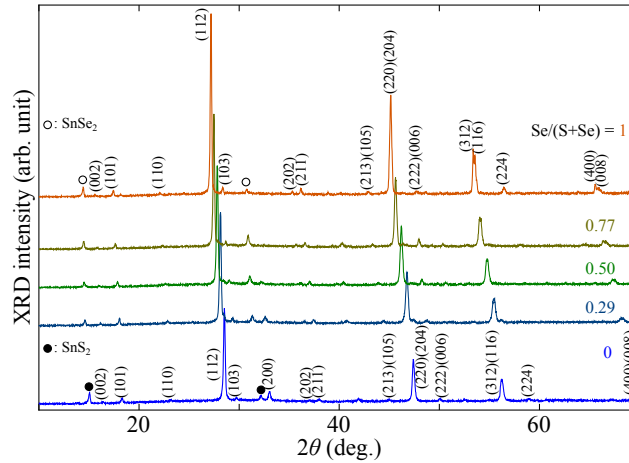


Fig. 1. XRD patterns of CZTSSe absorbers prepared at various Se/(S+Se) ratios. The Miller indices of CZTS and CZTSe crystals are shown beside each corresponding pattern.

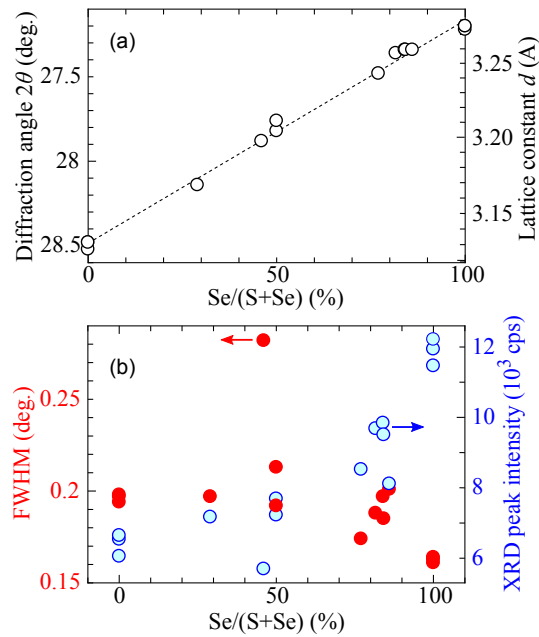


Fig. 2. Plots of (a) diffraction angle (2θ) and lattice constant of (112) planes, (b) FWHM and XRD intensity of (112) peak against the Se/(S+Se) ratios of CZTSSe absorbers.

detected by the XRD analysis, were dominantly located near the surface. A graph of lattice spacing of (112) planes versus Se/(S+Se) ratios is shown in Fig. 2(a). It is found that the lattice spacing was increased proportionally from 3.1314 to 3.2758 Å as the amount of selenium became larger. From these results, it can be considered that the CZTSSe alloys could be synthesized to have the same crystal structure as those of the CZTS and CZTSe host crystals over the whole compositional range without phase transformation, and following Vegard's law.¹⁷⁾ In comparing the FWHM as shown in

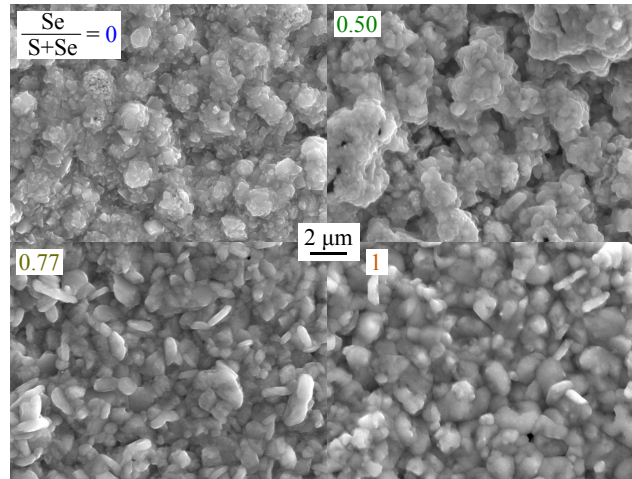


Fig. 3. SEM images of CZTSSe absorbers with various Se/(S+Se) ratios.

Fig. 2(b), it is found that the CZTSe thin film has a smaller FWHM value than the CZTS. This implies that the crystallinity of CZTSe, which could represent the size of the crystal grains, is superior. In the case of CZTSSe alloys, the distribution of FWHM values was observed, which may reflect the existence of the lattice strain due to the solid alloy, and/or the presence of the aggregation of minute crystals with different Se/(S+Se) ratios. On the other hand, the XRD peak intensity of the (112) plane was enhanced when the Se/(S+Se) ratio became larger, which it turn suggested the improvement of crystallinity. The surface morphologies of CZTSSe absorbers at various Se/(S+Se) ratios are shown in Fig. 3. It can be seen that the samples with higher selenium content have a larger grain size. This tendency was also in good agreement with the XRD analysis. The resistivity of the absorber film was decreased with increasing Se/(S+Se) ratio and was varied between 2×10^3 and $2.7 \times 10^2 \Omega \cdot \text{cm}$ nonlinearly. This could be due to the enhancement of the grain size and crystallinity so that the carrier mobility was improved.

The J - V characteristics of $\text{In}_2\text{O}_3/\text{CdS}/\text{CZTSSe}/\text{Mo}/\text{SLG}$ solar cells using the CZTSSe absorbers prepared in this experiment are described in Fig. 4. The improvement of the short-circuit current density J_{sc} in accordance with the increase of selenium content was observed, while the open-circuit voltage V_{oc} was dropped as a tradeoff to this. In the cell using CZTSe of Se/(S+Se)=1, it suffered a drastic reduction of the V_{oc} , which obviously lowered the conversion efficiency. The highest conversion efficiency of 4.22% was obtained from the cell with the $\text{Cu}_2\text{ZnSn}(\text{S}_{0.23}\text{Se}_{0.77})_4$ absorber. The largest J_{sc} of $31.67 \text{ mA}/\text{cm}^2$ was achieved, which is 2.5 times larger than that of the cell using a pure CZTS absorber. On the other hand, the V_{oc} was decreased by 40% compared with the cell with the CZTS absorber. The cross-sectional image of the cell with the $\text{Cu}_2\text{ZnSn}(\text{S}_{0.23}\text{Se}_{0.77})_4$ absorber is shown in Fig. 5. A continuous junction was identified along the whole CdS/CZTSSe interface. However, voids in the absorber layer as well as at the CZTSSe/Mo interface were quite obvious. This may be the main reason that deteriorated the performance of the cells. The corresponding normalized QE of the cells

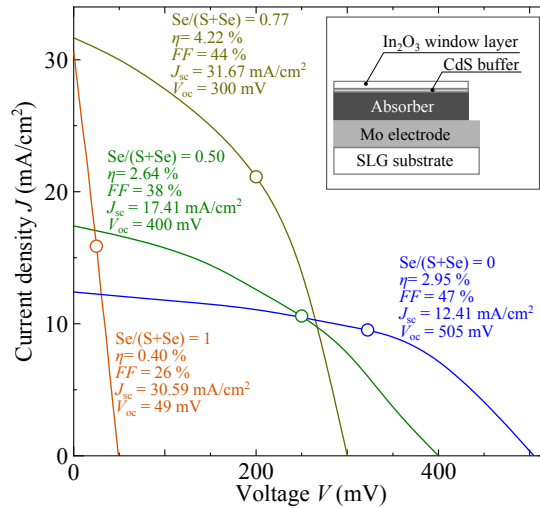


Fig. 4. J - V characteristics of thin-film solar cells with CZTSSe absorber having various Se/(S+Se) ratios.

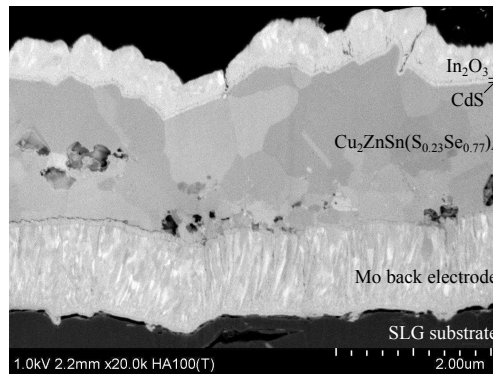


Fig. 5. Cross-sectional SEM image of thin-film solar cell using $\text{Cu}_2\text{ZnSn}(\text{S}_{0.23}\text{Se}_{0.77})_4$ absorber.

shown in Fig. 4 are depicted in Fig. 6. It is clearly observed that the extension of QE spectra into longer wavelength side was mainly due to the increase of the Se/(S+Se) ratio. This indicated that the absorption edge of the absorber layer was shifted to the lower energy side when the concentration of selenium was increased in the CZTSSe alloy. From the QE spectrum, the absorption edge of the $\text{Cu}_2\text{ZnSn}(\text{S}_{0.23}\text{Se}_{0.77})_4$ absorber was estimated to be about 1.1 eV. This value is close to the bandgap of the CZTSe thin film (about 1.0 eV) from previous reports.^{18,19)} The widening of the effective absorption range of the cell is considered to be a major factor that contributed to the improvement of J_{sc} discussed above. In the future, it is possible to tune the bandgap of the CZTSSe alloy for adjusting the bandgap alignment of the CdS/CZTSSe interface to realize an optimum photovoltaic performance.

Thin films of CZTSSe alloy were fabricated successfully by simultaneous reaction under the preset ratios of sulfur and selenium partial vapor pressures. The resultant compositional ratios of the films were close to that of the preset Se/(S+Se) ratios. The existence of the CZTSSe alloy in the form

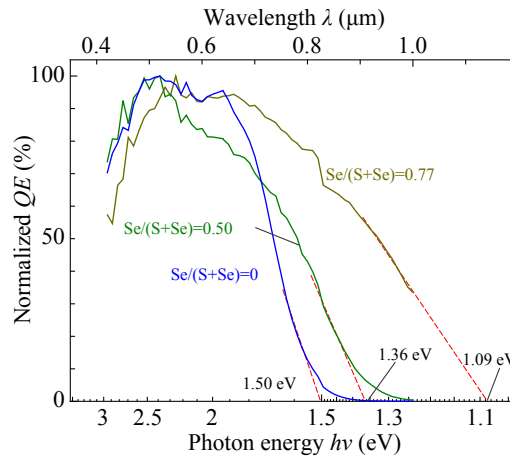


Fig. 6. Normalized QE of solar cells using CZTSSe absorbers with different $Se/(S+Se)$ ratios.

of a crystal phase similar to its host crystals of CZTS and CZTSe was confirmed over the whole compositional range. The lattice transformation of the CZTSSe alloy due to the change in selenium content was in good agreement with Vegard's law. The crystal grain size and electrical conductivity were enhanced when the $Se/(S+Se)$ ratio was increased. The photovoltaic conversion efficiency of the solar cell with a $Cu_2ZnSn(S_{0.23}Se_{0.77})_4$ absorber exhibited the highest short circuit current density of 31.67 mA/cm^2 among those with lower selenium contents. This could be considered as the benefit of effectively broadening the wavelength range of absorption by the solar cell. In contrast, a decrease in the open-circuit voltage was observed as a tradeoff.

Acknowledgment Special thanks are due to Mr. Isamu Minemura and Mr. Tomohiko Yamakami for their help in this study.

References

- 1) K. Ito and T. Nakazawa: *Jpn. J. Appl. Phys.* **27** (1988) 2094.
- 2) K. Ito and T. Nakazawa: *Proc. 4th Int. Conf. Photovoltaic Science and Engineering*, 1989, p. 341.
- 3) H. Katagiri, K. Jimbo, S. Yamada, T. Kamimura, W. S. Maw, T. Fukano, T. Ito, and T. Motohiro: *Appl. Phys. Express* **1** (2008) 041201.
- 4) B. Shin, O. Gunawan, Y. Zhu, N. A. Bojarczuk, S. J. Chey, and S. Guha: *Prog. Photovolt.: Res. Appl.* DOI: 10.1002/pip.1174 (2011).
- 5) D. A. R. Barkhouse, O. Gunawan, T. Gokmen, T. K. Todorov, and D. B. Mitzi: *Prog. Photovolt.: Res. Appl.* **20** (2012) 6.
- 6) K. Wang, O. Gunawan, T. Todorov, B. Shin, S. J. Chey, N. A. Bojarczuk, D. Mitzi, and S. Guha: *Appl. Phys. Lett.* **97** (2010) 143508.
- 7) B.-A. Schubert, B. Marsen, S. Cinque, T. Unold, R. Klenk, S. Schorr, and H.-W. Schock: *Prog. Photovolt.: Res. Appl.* **19** (2011) 93.
- 8) K. Tanaka, M. Oonuki, N. Moritake, and H. Uchiki: *Sol. Energy Mater. Sol. Cells* **93** (2009) 583.
- 9) M. Jiang, Y. Li, R. Dhakal, P. Thapaliya, M. Mastro, J. D. Caldwell, F. Kub, and X. Yan: *J. Photonics for Energy* **1** (2011) 019501.
- 10) A. Ennaoui, M. Lux-Steiner, A. Weber, D. Abou-Ras, I. Kotschau, H.-W. Schock, R. Schurr, A. Holzinger, S. Jost, R. Hock, T. Vos, J. Schulze, and A. Kirbs: *Thin Solid Films* **517** (2009) 2511.
- 11) Q. Guo, G. M. Ford, W.-C. Yang, B. C. Walker, E. A. Stach, H. W. Hillhouse, and R. Agrawal: *J. Am. Chem. Soc.* **132** (2010) 17384.
- 12) N. Momose, M. T. Htay, T. Yudasaka, S. Igarashi, T. Seki, S. Iwano, Y. Hashimoto, and K. Ito: *Jpn. J. Appl. Phys.* **50** (2011) 01BG09.
- 13) M. T. Htay, Y. Hashimoto, N. Momose, K. Sasaki, H. Ishiguchi, S. Igarashi, K. Sakurai, and K. Ito: *Jpn. J. Appl. Phys.* **50** (2011) 032301.
- 14) N. Meyer, I. Luck, U. Ruhle, J. Klaer, R. Klenk, M. Ch. Lux-Steiner, and R. Scheer: *Proc. 19th European Photovoltaic Solar Energy Conf.*, 2004, 4AO.9.6.
- 15) N. Meyer, A. Meeder, and D. Schmid: *Thin Solid Films* **515** (2007) 5979.
- 16) S. Y. Chen, X. G. Gong, A. Walsh, and S. H. Wei: *Appl. Phys. Lett.* **94** (2009) 041903.
- 17) A. R. Denton and N. W. Ashcroft: *Phys. Rev. A* **43** (1991) 3161.
- 18) S. Ahn, S. Jung, J. Gwak, A. Cho, K. Shin, K. Yoon, D. Park, H. Cheong, and J. H. Yun: *Appl. Phys. Lett.* **97** (2010) 021905.
- 19) I. Repins, C. Beall, N. Vora, C. DeHart, D. Kuciauskas, P. Dippo, B. To, J. Mann, W.-C. Hsu, A. Goodrich, and R. Noufi: *Sol. Energy Mater. Sol. Cells* **101** (2012) 154.